K. ŽIŽEK et al., High-shear vs. Fluid-bed Granulation Process of Dolomite: Process …, *Chem. Biochem. Eng. Q.* **25** (1) 1–8 (2011)

1

High-shear vs. Fluid-bed Granulation Process of Dolomite: Process Modeling

K. Žižek,* **M. Hraste, and Z. Gomzi**
Faculty of Chemical Engineering and Technology, University of Zagreb,
Marulićev trg 20, 10 000 Zagreb, Croatia

High-shear and fluid-bed processes were used for granulation of dolomite powder into agrochemical product. In this paper, comparative study of the granulation process focuses on the observation of granule size distribution (GSD). Considerable difference between high-shear and fluid-bed GSDs is analyzed with process kinetics. Simulation of dynamic development of GSD is achieved with application of a 1-D discretized population balance and Equi-Partition of Kinetic Energy (EKE) coalescence model. The used approach indicates for both processes (high-shear and fluid-bed granulation) the presence of coalescence growth as a dominant mechanism in the dolomite granulation process. Deviations between simulated and real GSDs signify the probable existence of other granulation mechanism(s). *A posteriori* approach by the integral method was used for coalescence rate constant estimation. The generated kinetic considerations represent a valuable step towards a comprehensive perspective of dolomite granulation and implementing the acquired knowledge in real-life agrochemical granulation.

Key words:
High-shear granulation, fluid-bed granulation, dolomite, granule size distribution, population balance

Introduction

Granulation is a size-enlargement process of transforming solid particles into particulate form with defined properties to meet the specific end use requirements. These properties include the size of a granule, its microstructure and its shape. Such primary properties effect the system rheology, the capability of eventual compacting, dissolution, hardness etc. Nowadays granulation is vital processing step in the manufacture of ceramics, pharmaceuticals, fertilizers, food products and biotechnology products as well. The most common process units utilized in the granulation process include high-shear mixer and fluidized bed. Each one has certain advantages and disadvantages.

Observing the process as a physical phenomenon, granulation stands as a complex couple of the elementary processes: nucleation, consolidation and growth, and breakage. The processes are transient and they all occur simultaneously in the granulation unit. Understanding granulation implies considering the contributions of all elementary processes. The process participation degree, influenced by operating conditions, formulation properties and the used granulation unit consequently determines final granule size distribution (GSD). A considerable effort was provided to investigate the influence of process variables and physicochemical properties on the granulation mechanisms and resulting GSDs

in high-shear[1–4] and fluid-bed process systems.[5–8] However, the greatest contribution to the mathematical perception of the dynamic evolution of the property of a group of granules was achieved by implementing population balance approach.

This paper investigates the dynamic evolution of the GSD for both process systems and the possibility of its simulation with the use of 1-D discretized form of population balance[9] and Equi-Partition of Kinetic Energy (EKE) model.[10]

Population balance as a statement of continuity for particulate systems[11] follows how the number of entities in the given size interval in detached process control volume will change during the process. Simultaneously participation of the several competing physical phenomena makes population balance modeling of granulation, tempting and demanding. Each granule system is characterized with three internal coordinates (v_S, v_L, v_G), one each for the concerned phase state. Therefore, a mechanistic approach to granulation necessarily demands application of 3-D population balance equation. According to Scott *et al.*,[12] at the very early stage of the process, the volume of gas phase in granule entity becomes negligible. If the assumption was made that all granules from a given size class at a given time contain the same binder composition, population balance is simplified to 1-D form. Considering well-mixed, batch process unit with the coalescence as the only process that changes the

---
*Corresponding author: E-mail address: kzizek@fkit.hr

observed property, the population balance equation becomes:

$$\frac{\partial n(t,v)}{\partial t} = \frac{1}{2} \int_0^v \beta(v-u,u) n(t,u) n(t,v-u) \, \mathrm{d}u - \\ - n(t,v) \cdot \int_0^\infty \beta(v,u) \, n(t,u) \, \mathrm{d}u \tag{1}$$

Significant progress in solving such a partial integro-differential equation was made by integrating the discretization technique in granulation considerations. Applying the M-I approach (the Mean value theorem on frequency), Hounslow et al.[9] introduced a discretized population balance for tracking the change in the number of particles in size interval i (N_i):

$$\frac{\mathrm{d}N_i}{\mathrm{d}t} = N_{i-1} \sum_{j=1}^{i-1} (2^{j-i+1} \beta_{i-1,j} N_j) + \frac{1}{2} \beta_{i-1,i-1} N_{i-1}^2 - \\ - N_i \sum_{j=1}^{i-1} (2^{j-i} \beta_{i,j} N_j) - N_i \sum_{j=i}^{i_{\max}} \beta_{i,j} N_j \tag{2}$$

where i and j are the size intervals of the colliding particles. Application of this equation in attempts to model the coalescence only granulation processes is tremendous.[13–19] The coalescence kernel is generally defined with two contributions:[20]

$$\beta(u,v,t) = \beta_0(t)\,\beta(u,v) \tag{3}$$

The first part, $\beta_0(t)$, is the coalescence rate constant, which involves the influence of operating conditions and formulation properties. The second part, $\beta(u,v)$ represents the influence of colliding entity sizes on the net coalescence rate. Various empirical and theoretical expressions for coalescence kernel, $\beta_{i,j}$, estimation have been brought and used in the literature. In this paper, Equi-Partition of Kinetic Energy (EKE) model:[10]

$$\beta_{i,j} = \beta_0 (d_i + d_j)^2 \sqrt{\frac{1}{d_i^3} + \frac{1}{d_j^3}} \tag{4}$$

was assumed. This model assumes that particles collide as a consequence of their random component of velocity and that the random components result in equal distribution of the particles' kinetic energy. This includes size dependence of the coalescence rate.

Experiment

Materials

The feed powder was dolomite (Kamen Sirač, d.d., Sirač, Croatia). Initial particle size distribution

(PSD) was determined in wet mode applying laser diffraction method (Mastersizer 2000, Malvern Instruments, UK). PSD is displayed via volume density function (Fig. 1). Attained diameter means were: $d_{3,2}$ of 9.67 μm and $d_{4,3}$ of 38.44 μm.
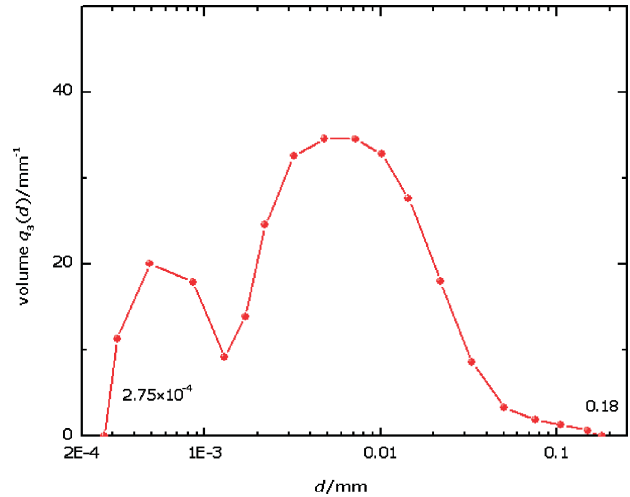

F i g . 1 – *Feed particle size distribution*

A three-component system water-molasses-polyvinylpyrrolidone K30 (*Plasdone*) was used as a binder formulation. In each experiment, mass portions of certain components in the binder system were kept constant (58 % water, 25 % molasses, 17 % PVP).

High-shear mixer

High-shear granulation experiments were performed in a Pharma Mixer P 1–6 (Diosna Dierks & Sohne, GmbH, Germany), vertical axis, high-shear mixer, of a capacity of 4 L (Fig. 2a). This granulator is equipped with two rotating elements: the impeller (design B 14 S), which was vertically mounted at the bottom of the bowl, and horizontally mounted chopper (design IM 2302). Speed intensity of the rotating elements was maintained constant during the entire granulation process.

Fluid-bed process unit

Fluid-bed granulation experiments were carried out in the lab-scale fluidized bed unit (Uni-Glatt, Glatt GmbH, Binzen, Germany), using a top-spray arrangement (Fig. 2b). Before entering the powder bed, the fluidizing air is preheated. The binder solution is delivered to the powder bed from the top through a two-fluid nozzle (Schlick) fed by a peristaltic pump. The liquid flow rate is controlled by the pump revolution setting.
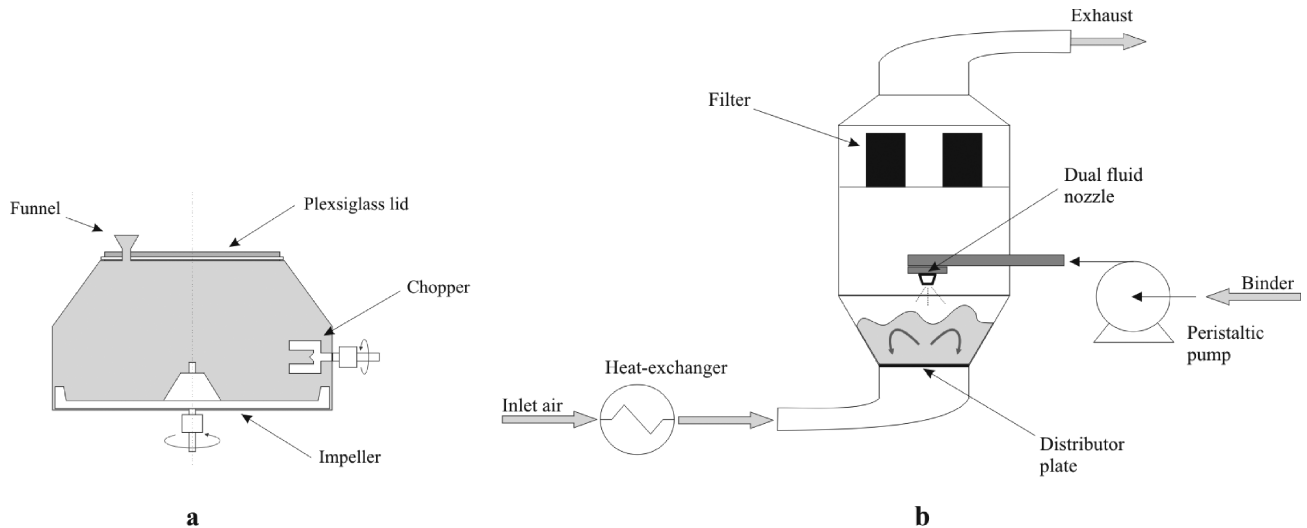
F i g . 2 – *Schematic of: a) high-shear mixer granulator, b) fluid-bed granulator*

High-shear granulation process

The temperature in the mixer granulator unit was constant. Dolomite powder was weighed and freely hand poured into the granulator. A certain amount of the binder formulation was poured manually in order to achieve the desirable liquid-to-solid mass ratio, L/S. A pre-mixing stage in these experiments did not exist. Mixing time was a variable parameter in this set of experiments. Afterwards, the granule population was dried in the Fluidized bed drier (Diosna Dierks & Sohne, GmbH, Germany). Experiments were performed at conditions summarized in Table 1.

T a b l e 1 – *Process parameters of high-shear granulation*

Parameter	Value	Unit
binder addition	pour-on	–
drying temperature	50 inlet 25 product	°C
feed mass	0.4	kg
granulation time	15, 30, 45, 60, 75, 90	s
impeller/chopper speed	300/1200	rpm
liquid-to-solid ratio	0.15	–
process unit temperature	25	°C

Fluid-bed granulation process

Each fluid-bed granulation experiment followed the next sequence:

– *Heating the fluidization chamber up to steady-state temperature* with the air of constant inlet temperature. Indicator for achieved steady state is a constant outlet gas temperature.

– *Granulation process* was accomplished by adding the binder formulation on powder bed. During one granulation experiment, all process parameters were kept constant.

– *After-drying of material* to constant outlet gas temperature.

Fluid-bed experiments were carried out at conditions summarized in Table 2.

T a b l e 2 – *Process parameters of fluid-bed granulation*

Parameter	Value	Unit
atomizing air pressure	0.8	bar
bed mass	0.4	kg
granulation time	15, 30, 45, 60, 75, 90	s
inlet air temperature	50	°C
liquid-to-solid ratio	0.15	–
nozzle aperture diam.	0.8	mm
outlet gas temperature	25	°C
rate of binder addition	40	g min^{-1}

Particle size distribution of derived granules was measured using the sieving technique (ASTM E11–95). GSD was reported via normalised mass density function, $q_3(d)$.

Granulation experiments were repeated in order to examine the ability of GSD reproducibility. Discrepancy among GSDs was reported as the sum of squared errors (SSE).

Modeling

To explore the suitability of the mentioned mechanistic approach[9,10] for simulating granulation of dolomite, fifteen ordinary differential equations (eq. 2) were derived, one for each concerned size interval, i (Table 3). The displayed size intervals and their ranges were defined with the sieve selection. A set of fifteen ordinary differential equations was numerically solved using the Runge-Kutta method (provided with Matlab software). In the model testing procedure, simulated and experimental GSDs were introduced as number size distributions. Representation of such distributions was enabled with the use of differential form of number cumulative function, $dQ_0(d)$ which stands as a number content of entities in size interval i.

T a b l e 3 – *Used size intervals, i*

Interval	Size range/mm	Interval	Size range/mm	Interval	Size range/mm
1	0.090–0	6	0.850–0.710	11	3.350–2.360
2	0.125–0.090	7	1.180–0.850	12	4.000–3.350
3	0.180–0.125	8	1.400–1.180	13	5.600–4.000
4	0.355–0.180	9	1.700–1.400	14	6.700–5.600
5	0.710–0.355	10	2.360–1.700	15	8.000–6.700

Estimation of the β_0 parameter was enabled by integral approach, minimizing the sum of squared errors (SSE) between the simulated and experimental results:

$$\mathrm{SSE} = \sum_t \sum_i (dQ_0(d) - d\hat{Q}_0(d))^2 \qquad (5)$$

Results and discussion

Fig. 3 shows the dynamic evolution of the GSD for diverse granulation systems.

Heterogeneity behavior was discovered in each high-shear GSD (Fig. 3a). Such bimodal and multimodal appearance of the GSD was also reported in previous studies of other pour-on, high-shear granulations,[12,14] where the formulation used was also of carbonatic constitution ($CaCO_3$). Physical explanation for such size distribution pattern of dolomite entities was discovered in the Schaefer and Mathiesen Immersion Hypothesis (SMIH).[12] According to SMIH theory, appearance of distribution peak at lower diameter ranges (mostly at 0.1075 mm) is due to residual coarse initial particles. They have a much lower probability of leading to coalescence than fines in primary monomodal distribution.
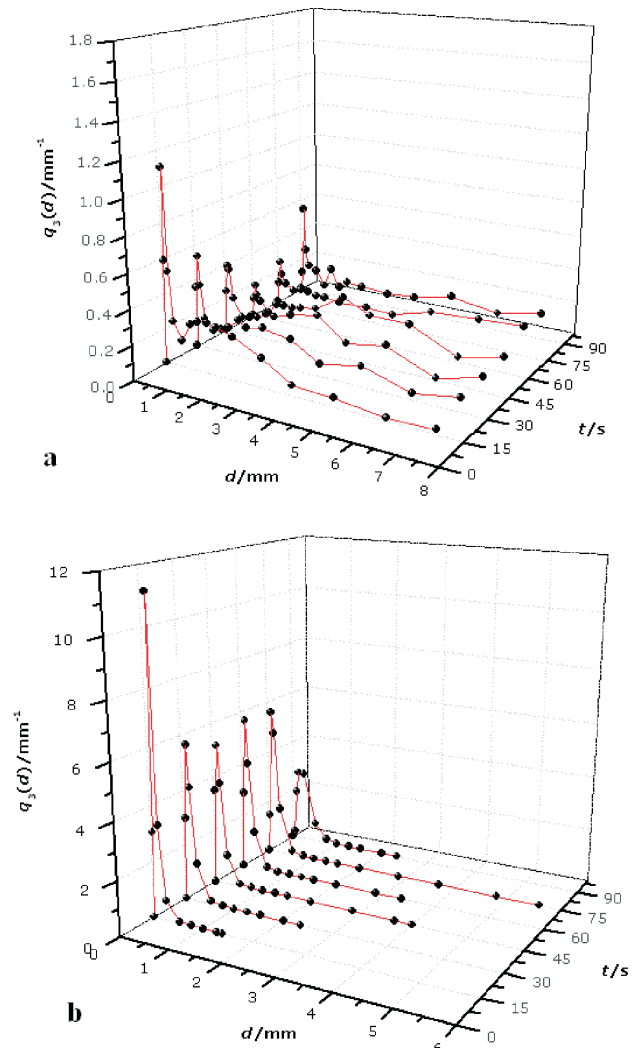

F i g . 3 – *Dynamic evolution of experimental GSD at early stage of: a) high-shear granulation, b) fluid-bed granulation*

Fluid-bed granulation tests yield with monomodal and narrow GSDs (Fig. 3b). Such significant narrowness of GSD and presence of smaller granules with respect to high-shear GSDs are consistent with former fluid-bed studies.[5–7,21–23] Furthermore, non-heterogeneity behavior in fluid-bed GSDs is quite opposite to those found in high-shear GSDs. Higher entity degradation rates in fluid-bed units[18] were found as a major contributor to non-sustainability of SMIH theory.[12] In order to completely clarify such GSD formation it is inevitable to consider simultaneity of drying process.

Slight discrepancies, observed among GSDs, indicate potential reproducibility of the granulation experiments for both lab-scale units (Fig. 4). For high-shear granulation test at 300 rpm mixer speed ($t = 75$ s) SSE equals 0.050 (Fig. 4a) and for fluid-bed test at identical process time SSE amounts 0.034 (Fig. 4b).
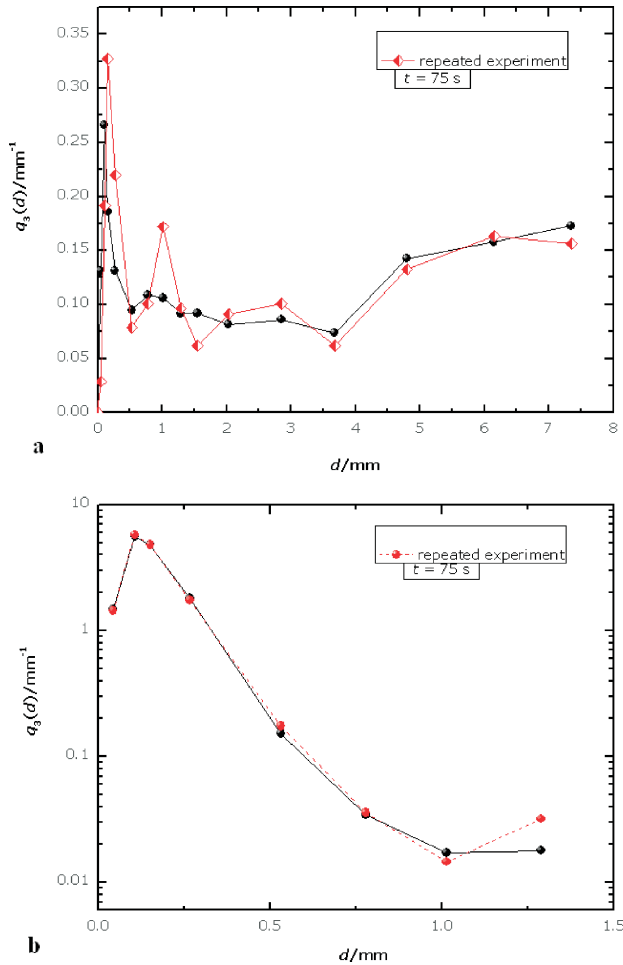
F i g . 4 – *Potential reproducibility for: a) high-shear granulation experiments, b) fluid-bed granulation experiments*

Recognizable pattern of the GSD for each process system[5–7,12,14,21–23] is already detected at the early stage of the process. We believe that GSDs would certainly change with time after 90 s until steady-state of the granulation process. However, distinguishing pattern of the GSD for both processes (wideness/narrowness, heterogeneity/non-heterogeneity behavior, presence of bigger/smaller entities) will remain time unchangeable. Thereby, the GSDs obtained at the early stage of the process (15–90 s) become quite sufficient criteria in equipment selection procedure. Therefore, if a presence of bigger dolomite entities with wide GSD is required, recommendation will be working with high-shear granulator, whereas for production of smaller dolomite entities with narrow GSD, fluid-bed unit should be suggested for granulation process.

Question arises: Can our reported GSDs be simulated within the time used (15–90 s) with 1-D population balance[9] considering the fact that its derivation from 3-D model is allowed only for times beyond very early stage of the process?[12]

Model testing

Figs. 5 and 6 show the ability of GSD simulation with the application of the mechanistic approach modeling. It demonstrated a good agreement between the experimental and simulated results. Such observation was given for both granulation processes. Divergence among experimental results and those derived by modeling technique is reported via SSE. The values of SSE (Table 4) are slightly different. A better fit of the model was achieved for the high-shear granulation process.

The modeled results suggest that dolomite entities in high-shear mixer and fluid-bed unit grow by coalescence granulation mechanism. However, the presence of a measurable discrepancy might be quantitative evidence for the additional participation of other granulation mechanism(s) (e.g. nucleation and breakage). These observations are logical; hence the applied model[9] is valid with the essential assumption that the coalescence is only active mechanism in the granulation unit. Therefore, coalescence as the dominant granulation mechanism, accompanied by other simultaneous mechanism(s), is present at the early stage (15–90 s) of the high-shear and fluid-bed granulation process of dolomite.

Implying thesis of Scott *et al.*[12] which tolerates simplification of 3-D population balance into 1-D model for the case of "non-early" process times, good simulation results possibly reveal proximate time at which dolomite granules become gasless. Also, integration of the EKE model[10] in simulation results marks coalescence rate of dolomite as size dependent parameter.

Parameter β_0 estimation was accomplished by minimizing the overall sum of squared errors (eq. 5) between the simulated and experimental results. The coalescence rate constants, β_0 (Table 4) are independent of the employed times within the early granulation stage (15–90 s). Some difference between constants obtained in various process units was observed. The order of magnitude of β_0 parameters (10^{-5}, 10^{-4} m$^{-1/2}$ s^{-1}) in these granulation tests is considerably higher than those reported in previous kinetic studies of the granulation process.[14,17] Explanation for this can be found in diverse formulations used. Additional experiments must be provided in order to quantitatively argument such a premise.

T a b l e 4 – *Model parameters*

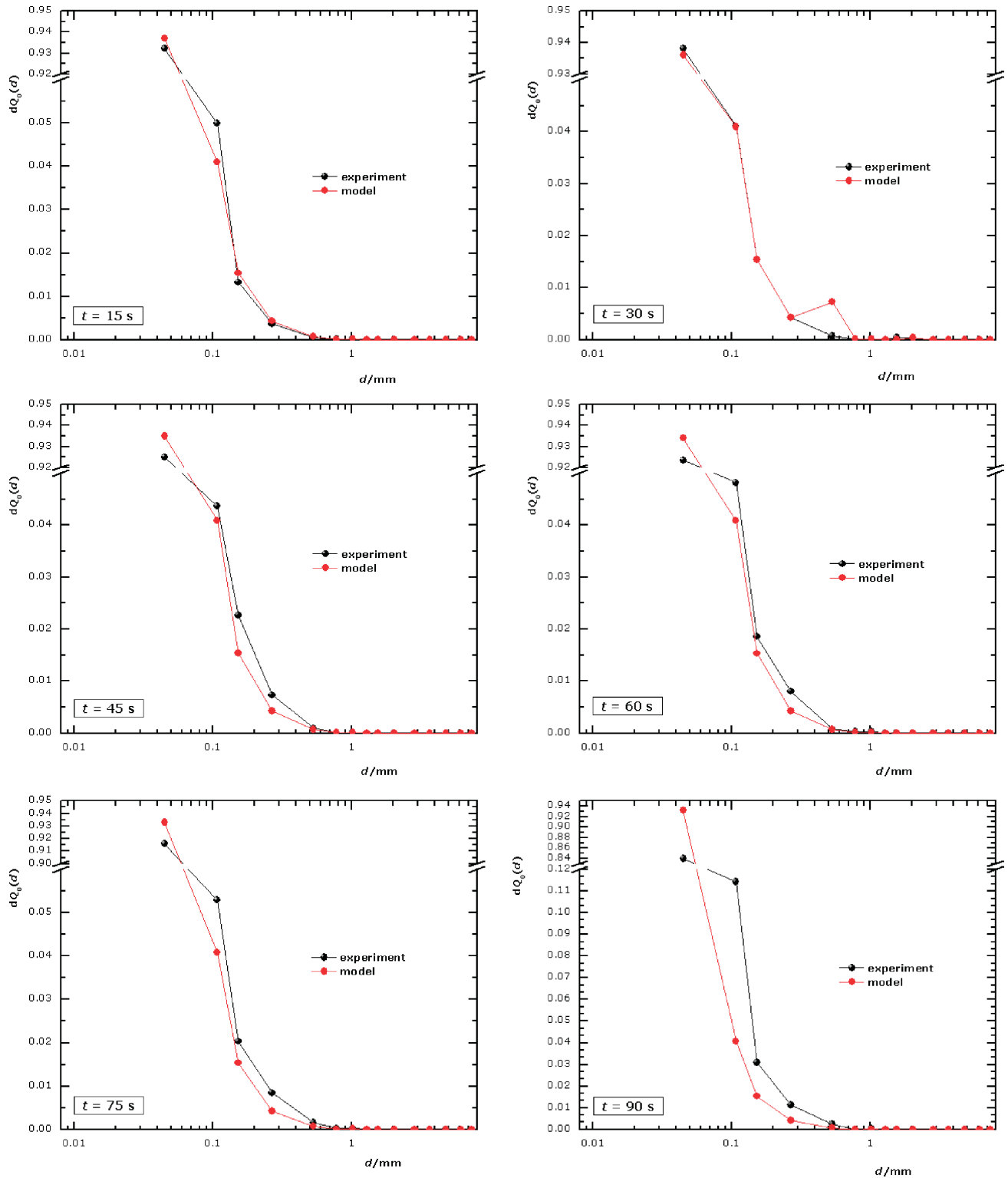| Granulation device	β_0/m$^{-1/2}$ s^{-1}	SSE
high-shear mixer	$1.583 \cdot 10^{-4}$	$1.365 \cdot 10^{-3}$
fluid-bed unit	$2.12 \cdot 10^{-5}$	$3.645 \cdot 10^{-3}$

F i g . 5 − *The fit of number size distribution (number content of entities in size interval i) with discretized PBE and EKE model for early stage of high-shear granulation process*
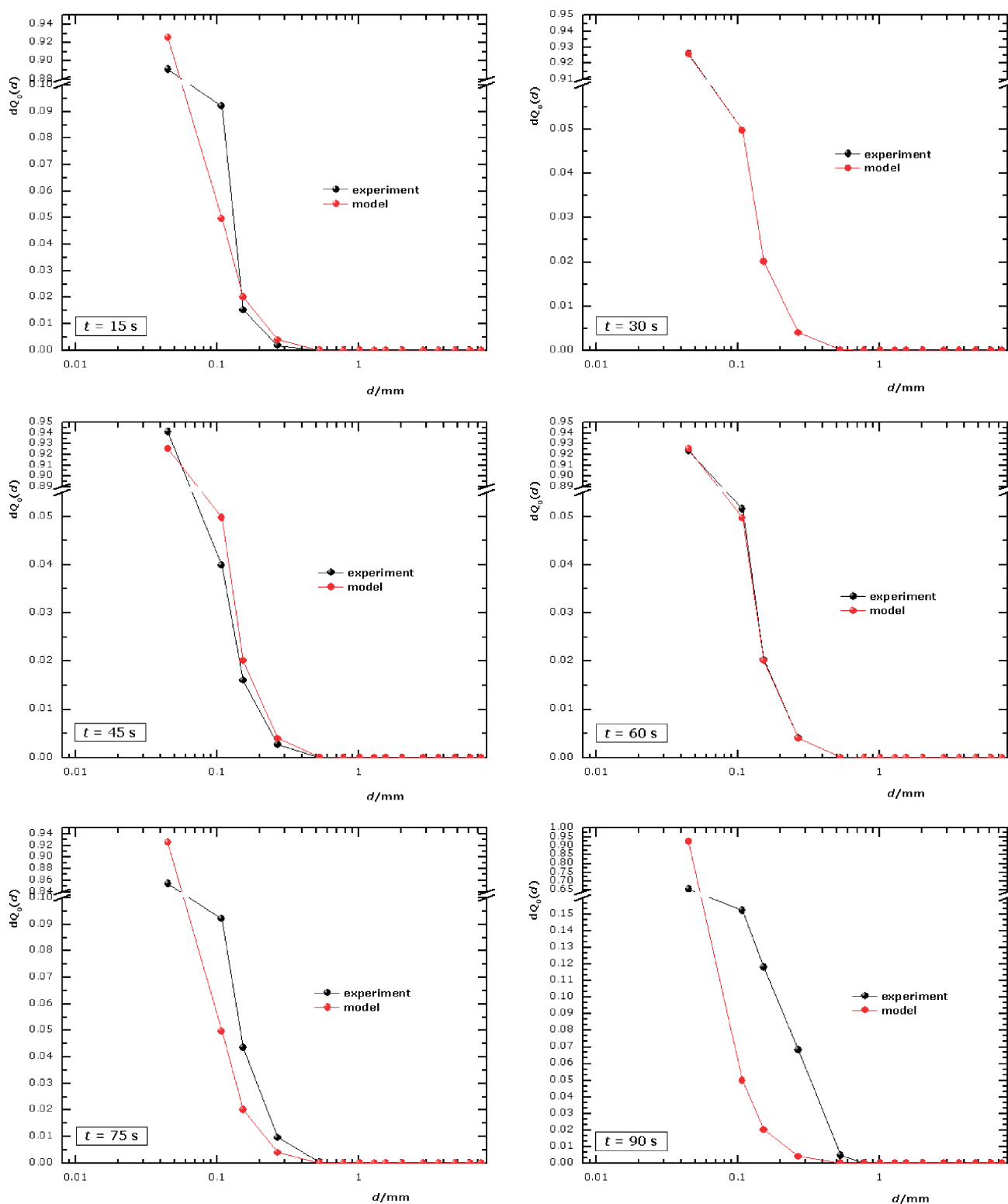
F i g . 6 – *The fit of number size distribution (number content of entities in size interval i) with discretized PBE and EKE model for early stage of fluid-bed granulation process*

Conclusions

High-shear granulation of dolomite for used process times (15–90 s) yields with wide and bi-modal or multimodal GSDs. For identical process times fluid-bed granulation produces narrow and monomodal GSDs. Such a recognizable pattern of the GSD for both process systems, noticed already at the early stage of the process, is time unchangeable. Therefore, early GSDs stand as one of the criteria in the process system selection procedure.

The simulation procedure provided by the discretized form of one-dimensional population balance model and EKE coalescence model was tested. A good agreement between experimental and simulated results was achieved. The used modeling procedure successfully describes and predicts the GSD at the early stage of a dolomite high-shear and fluid-bed granulation process.

Such a mechanistic approach can be used as an indicator of coalescence as a dominant granulation mechanism. Minor deviations between simulated and experimental results indicate the probability of existence of other granulation mechanism(s). More tracer experiments should be carried out to determine their degree of participation.

The rate of coalescence was quantified with the integral method. The results show that there is a notable difference between the coalescence rates obtained for high-shear and fluid-bed process system.

Good simulation results with EKE integrated coalescence model also imply size dependence of the coalescence rate.

Nomenclature

d – particle size, m

$d_{3,2}$ – Sauter mean diameter, m

$d_{4,3}$ – De Brouckere mean diameter, m

d_i – particle size in size class i, m

d_j – particle size in size class j, m

L – binder mass, kg

$n(v)$ – number density function, kg^{-1} m^{-1}

N_i – number of particles in size interval i

$q_3(d)$ – normalized mass probability density function, m^{-1}

$dQ_0(d)$ – experimental data for number content of entities in size interval i

$d\hat{Q}_0(d)$ – simulated data for number content of entities in size interval i

S – feed powder mass, kg

SSE – sum of squared errors

t – time, s

u – granule volume, m^3

v – granule volume, m^3

v_G – volume of air, m^3

v_L – volume of liquid, m^3

v_S – volume of solid, m^3

Greek letters

$\beta_{i,j}$ – coalescence kernel, s^{-1}

β_0 – coalescence rate constant, m$^{-1/2}$ s^{-1}

References

1. *Knight, P. C., Instone, T., Pearson, J. M. K., Hounslow, M. J.,* Powder Technol. **97** (1998) 246.

2. *Saleh, K., Vialatte, L., Guigon, P.,* Chem. Eng. Sci. **60** (2005) 3763.

3. *Schaefer, T., Johnsen, D., Johansen, A.,* Eur. J. Pharm. Sci. **21** (2004) 525.

4. *Bock, T. K., Kraas, U.,* Eur. J. Pharm. & Biopharm. **52** (2001) 297.

5. *Boerefijn, M. J., Hounslow, M. J.,* Chem. Eng. Sci. **60** (2005) 3879.

6. *Cryer, S. A., Scherer, P. N.,* AIChE J. **49** (2003) 2802.

7. *Pont, V., Saleh, K., Steinmetz, D., Hemati, M.,* Powder Technol. **120** (2001) 97.

8. *Rajniak, P., Mancinelli, C., Chern, R., Stepanek, F., Farber, L., Hill, B.,* Int. J. Pharm. **334** (2007) 92.

9. *Hounslow, M. J., Ryall, R. L., Marshall, V. R.,* AIChE J. **34** (1988) 1821.

10. *Hounslow, M. J.,* The Population Balance as a Tool for Understanding Particle Rate Processes, Kona (1998) 179.

11. *Randolph, A., Larson, M.,* Theory of Particulate Processes: Analysis and Techniques of Continuous Crystallization, NY. Academic Press, New York, 1971.

12. *Scott, A. C., Hounslow, M. J., Instone, T.,* Powder Technol. **113** (2000) 205.

13. *Adetayo, A. A., Ennis, B. J.,* AIChE J. **43** (1997) 927.

14. *Biggs, C. A., Sanders, C., Scott, A. C., Willemse, A. W., Hoffman, A. C., Instone, T., Salman, A. D., Hounslow, M. J.,* Powder Technol. **130** (2003) 162.

15. *Darelius, A., Rasmuson, A., Bjorn, I. N., Folestad, S.,* Powder Technol. **160** (2005) 209.

16. *Hounslow, M. J., Pearson, J. M. K., Instone, T.,* AIChE J. **47** (2001) 1984.

17. *Le, P. K., Avontuur, P., Hounslow, M. J., Salman, A. D.,* Powder Technol. **189** (2009) 149.

18. *Peglow, M., Kumar, J., Warnecke, G., Heinrich, S., Morl, L.,* Chem. Eng. Sci. **61** (2006) 282.

19. *Sanders, C. F. W., Willemse, A. W., Salman, A. D., Hounslow, M. J.,* Powder Technol. **138** (2003) 18.

20. *Sastry, K. V. S.,* Int. J. Miner. Process. **2** (1975) 187.

21. *Bouffard, J., Kaster, M., Dumont, H.,* Drug Devel. Ind. Pharm. **31** (2005) 923.

22. *Peglow, M., Kumar, J., Heinrich, S., Warnecke, G., Tsotsas, E., Morl, L., Wolf, B.,* Chem. Eng. Sci. **62** (2007) 513.

23. *Saleh, M., Steinmetz, M., Hemati, M.,* Powder Technol. **130** (2003) 116.